

Random coincidence of $2\nu 2\beta$ decay events as a background source in bolometric $0\nu 2\beta$ decay experiments

D.M. Chernyak^{1,2}, F.A. Danevich¹, A. Giuliani^{2,a}, E. Olivieri², M. Tenconi², V.I. Tretyak¹

¹Institute for Nuclear Research, MSP, 03680 Kyiv, Ukraine

²Centre de Spectrométrie Nucléaire et de Spectrométrie de Masse, 91405 Orsay, France

Received: 8 March 2012 / Revised: 27 March 2012 / Published online: 24 April 2012

© The Author(s) 2012. This article is published with open access at Springerlink.com

Abstract Two-neutrino double β decay can create an irremovable background even in high energy resolution detectors searching for neutrinoless double β decay due to random coincidence of $2\nu 2\beta$ events in the case of poor time resolution. Some possibilities for suppressing this background in cryogenic scintillating bolometers are discussed. It is shown that the present bolometric detector technologies enable one to control this form of background at the level required to explore the inverted hierarchy of the neutrino mass pattern, including the case of bolometers searching for the neutrinoless double β decay of ^{100}Mo , which is characterized by a relatively short two-neutrino double β decay half-life.

1 Introduction

Neutrinoless double beta ($0\nu 2\beta$) decay is a key process in particle physics, since it provides the only experimentally viable possibility to test the Majorana nature of the neutrino and the lepton number conservation, establishing in the meantime the absolute scale and the hierarchy of the neutrino masses [1–3].

One of the most important goals of the next generation double β decay experiments is to explore the inverted hierarchy of the neutrino masses. In the inverted scheme the effective Majorana $\langle m_\nu \rangle$ neutrino mass is expected to be in the interval $\sim 0.02\text{--}0.05$ eV. In order to check this range, an experimental sensitivity (in terms of half-life) for the most promising nuclei should be at the level $T_{1/2} \sim 10^{26}\text{--}10^{27}$ yr. This requires a detector containing a large number of studied nuclei ($\sim 10^{27}\text{--}10^{28}$), with high energy resolution (at most a few percent at the energy of the decay $Q_{2\beta}$), large (ideally 100 %) detection efficiency, and very low (ideally zero) radioactive background.

Besides the high-purity germanium (HPGe) detectors used to search for $0\nu 2\beta$ decay of ^{76}Ge [4, 5], cryogenic bolometers [6, 7]—luminescent [8–12] or not [13–15]—are excellent candidates to realize large-scale high-sensitivity experiments involving different isotopes with high energy resolution (a few kiloelectron volts) and detection efficiency (near 70 %–90 %, depending on the crystal composition and size).

The Cryogenic Underground Observatory for Rare Events (CUORE) cryogenic experiment [14, 15], built on the successful Cuoricino and searching for $0\nu 2\beta$ decay of ^{130}Te with the help of TeO_2 detectors, is by far the most advanced bolometric search and is under construction now, while several searches (including LUCIFER [16] and AMoRE [17]), aiming to use different luminescent bolometers to search for double β decay of ^{82}Se (ZnSe [16, 18]), ^{116}Cd (CdWO_4 [19]), ^{100}Mo (CaMoO_4 [17] and ZnMoO_4 [20–23]), and ^{130}Te (TeO_2 [24]) are in the R&D stage.

However, a disadvantage of cryogenic bolometers is their poor time resolution. This can lead to a background component at the energy $Q_{2\beta}$ due to random coincidences of lower energy signals, especially those due to the unavoidable two-neutrino double β decay ($2\nu 2\beta$) events.

The random coincidence of $2\nu 2\beta$ events as a source of background in high-sensitivity $0\nu 2\beta$ experiments was considered and discussed for the first time in [22]. In this work, the contribution of random coincidences (rc) of $2\nu 2\beta$ events to the counting rate in the energy region of the expected $0\nu 2\beta$ peak is estimated. Methods to suppress the background are discussed.

2 Random coincidence of $2\nu 2\beta$ events

The energy spectra of β particles emitted in $2\nu 2\beta$ decay are related to the two-dimensional distribution $\rho_{12}(t_1, t_2)$ (see, e.g., [25] and references therein)

^a e-mail: andrea.giuliani@csnsm.in2p3.fr

$$\rho_{12}(t_1, t_2) = e_1 p_1 F(t_1, Z) \cdot e_2 p_2 F(t_2, Z) \cdot (t_0 - t_1 - t_2)^5, \tag{1}$$

where t_i is the kinetic energy of the i -th electron (all energies here are in units of the electron mass m_0c^2), t_0 is the energy available in the 2β process, p_i is the momentum of the i -th electron $p_i = \sqrt{t_i(t_i + 2)}$ (in units of m_0c), and $e_i = t_i + 1$. The Fermi function $F(t, Z)$, which takes into account the influence of the electric field of the nucleus on the emitted electrons, is defined as

$$F(t, Z) = \text{const} \cdot p^{2s-2} \exp(\pi\eta) |\Gamma(s + i\eta)|^2, \tag{2}$$

where $s = \sqrt{1 - (\alpha Z)^2}$, $\eta = \alpha Ze/p$, $\alpha = 1/137.036$, Z is the atomic number of the daughter nucleus ($Z > 0$ for $2\beta^-$ and $Z < 0$ for $2\beta^+$ decay), and Γ is the gamma function.

The distribution $\rho(t)$ for the sum of electron energies $t = t_1 + t_2$ is obtained by integration:

$$\rho(t) = \int_0^t \rho_{12}(t - t_2, t_2) dt_2. \tag{3}$$

This distribution is shown for ^{100}Mo in Fig. 1.

The Primakoff–Rosen (PR) approximation for the Fermi function $F(t, Z) \sim e/p$ [26], which is adequate for $Z > 0$, allows us to simplify Eq. (1) to the expression

$$\rho_{12}^{\text{PR}}(t_1, t_2) = (t_1 + 1)^2 (t_2 + 1)^2 (t_0 - t_1 - t_2)^5 \tag{4}$$

and to obtain the formula for $\rho(t)$ analytically:

$$\rho^{\text{PR}}(t) = t(t_0 - t)^5 (t^4 + 10t^3 + 40t^2 + 60t + 30). \tag{5}$$

The energy distribution for two randomly coincident $2\nu 2\beta$ decays $\rho_{\text{rc}}(t)$ can be obtained by numerical convolution

$$\rho_{\text{rc}}(t) = \int_0^t \rho(t - x)\rho(x) dx, \tag{6}$$

or with a Monte Carlo method by sampling energy releases in two independent $2\nu 2\beta$ events in accordance with the distribution (3) and adding them. The energy spectrum obtained by sampling 10^8 coincident $2\nu 2\beta$ events for ^{100}Mo is shown in Fig. 1. (We assume here an ideal energy resolution of the detector.) This distribution can be approximated by the following compact expression,¹ similar to that reported in Eq. (5):

$$\rho_{\text{rc}}(t) = t^3 (2t_0 - t)^{10} \sum_{i=0}^8 a_i t^i. \tag{7}$$

However, the coefficients a_i are different for different isotopes; for ^{82}Se , ^{100}Mo , ^{116}Cd , ^{130}Te (which are the nearest aims of the bolometric 2β experiments), they are given in Table 1. The approximation for ^{100}Mo is shown in Fig. 1.

¹One can expect a polynomial of 21st degree because of the formulae (5) and (6).

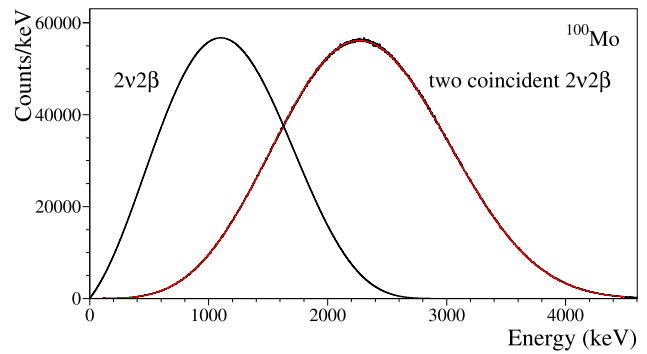


Fig. 1 Distribution for the sum of energies of two electrons emitted in $2\nu 2\beta$ decay of ^{100}Mo and energy spectrum of 10^8 two randomly coincident $2\nu 2\beta$ events for ^{100}Mo obtained by Monte Carlo sampling. The approximation of the random coincidence spectrum by the expression (7) is shown by the solid (red) line (Color figure online)

Table 1 Coefficients a_i in the energy distribution (7) for two randomly coincident $2\nu 2\beta$ events for ^{82}Se , ^{100}Mo , ^{116}Cd , and ^{130}Te

a_i	Isotope			
	^{82}Se	^{100}Mo	^{116}Cd	^{130}Te
a_0	3446.59	5827.48	20093.8	15145.6
a_1	-7746.37	-14399.7	-1318.65	5554.78
a_2	22574.7	34128.1	69134.6	39930.0
a_3	-16189.1	-23815.5	-31971.3	-13338.5
a_4	8467.01	11271.7	17976.8	7689.45
a_5	-2156.83	-2711.31	-3486.40	-813.887
a_6	337.172	390.396	406.762	-80.3126
a_7	-28.9146	-30.8774	-30.5846	19.1035
a_8	1	1	1	-1

The random coincidence counting rate I_{rc} in a chosen energy interval ΔE is determined by the time resolution of the detector τ and the counting rate for single $2\nu 2\beta$ events I_0 :

$$I_{\text{rc}} = \tau \cdot I_0^2 \cdot \varepsilon = \tau \cdot \left(\frac{\ln 2 N}{T_{1/2}^{2\nu 2\beta}} \right)^2 \cdot \varepsilon, \tag{8}$$

where N is the number of 2β decaying nuclei under investigation, and ε is the probability of registration of events in the ΔE interval. In Eq. (8) and in the following, we assume that if two events occur in the detector within a temporal distance lower than the time resolution τ , they give rise to a single signal with an amplitude equal to the sum of the amplitudes expected for the two separated signals. The calculated probabilities at the energy $Q_{2\beta}$ of the $0\nu 2\beta$ decay for the $\Delta E = 1$ keV interval are equal to $\varepsilon = 3.5 \times 10^{-4}$ for ^{82}Se and $\varepsilon = 3.3 \times 10^{-4}$ for ^{100}Mo , ^{116}Cd , and ^{130}Te .

Counting rates of detectors with 100 cm^3 volume (typical for large mass bolometers) at the energy of $0\nu 2\beta$ decay for different 2β candidates and compounds are presented in Table 2. We assume 100 % isotopical enrichment for ^{82}Se ,

Table 2 Counting rate of two randomly coincident $2\nu 2\beta$ events in cryogenic Zn^{82}Se , $^{40}\text{Ca}^{100}\text{MoO}_4$, $\text{Zn}^{100}\text{MoO}_4$, $^{116}\text{CdWO}_4$, and TeO_2 detectors of 100 cm^3 volume. Enrichment of ^{82}Se , ^{100}Mo , and ^{116}Cd is assumed to be 100 %, while for Te the natural isotopic abundance (34.08 %) is taken. C is the mass concentration of the isotope of inter-

est, ρ is the density of the material (g/cm^3), N is the number of 2β candidate nuclei in one detector, and B_{rc} is the counting rate at $Q_{2\beta}$ (counts/(keV·kg·yr)) under the assumption of 1 ms time resolution of the detector

Isotope	$T_{1/2}^{2\nu 2\beta}$ (yr) [27]	Detector (ρ)	C	N	B_{rc}
^{82}Se	9.2×10^{19}	Zn^{82}Se (5.65)	55.6 %	2.31×10^{24}	5.9×10^{-6}
^{100}Mo	7.1×10^{18}	$^{40}\text{Ca}^{100}\text{MoO}_4$ (4.35)	49.0 %	1.28×10^{24}	3.8×10^{-4}
		$\text{Zn}^{100}\text{MoO}_4$ (4.3)	43.6 %	1.13×10^{24}	2.9×10^{-4}
^{116}Cd	2.8×10^{19}	$^{116}\text{CdWO}_4$ (8.0)	31.9 %	1.32×10^{24}	1.4×10^{-5}
^{130}Te	6.8×10^{20}	TeO_2 (5.9)	27.2 %	0.76×10^{24}	1.1×10^{-8}

^{100}Mo , and ^{116}Cd , and natural abundance (34.08 %) for ^{130}Te . The time resolution of a detector is assumed as $\tau = 1$ ms. The reported rates scale linearly with the time resolution.

The background B_{rc} caused by random coincidences of $2\nu 2\beta$ events has the following dependence on the energy resolution R , the volume of the detector V , and the abundance or enrichment δ of the candidate nuclei contained in the detector:

$$B_{rc} \sim \tau \cdot R \cdot (T_{1/2}^{2\nu 2\beta})^{-2} \cdot V^2 \cdot \delta^2. \tag{9}$$

One can conclude from Table 2 that the most important random coincidence background is for ^{100}Mo due to its relatively short $2\nu 2\beta$ half-life. However, a non-negligible contribution is also expected for other isotopes for a large volume and poor time resolution of the single detectors.

Obviously, any other source of background with high enough energy can contribute due to random coincidences. For example, the presence of ^{234m}Pa (belonging to the series of ^{238}U) with a relatively high activity of 1 mBq/kg in 100 cm^3 ZnMoO_4 crystal will result in additional background due to random coincidence with $2\nu 2\beta$ events of 3.8×10^{-5} counts/(keV·kg·y) at ^{100}Mo $Q_{2\beta}$ energy. However, this contribution is much less important than that due to the $2\nu 2\beta$ decay alone. In addition, our simulations show that coincidence of $2\nu 2\beta$ signals with low energy events is not problematic, because of the quite steep shape of the $2\nu 2\beta$ spectrum near $Q_{2\beta}$. Low energy signals due to spurious sources, like microphonic noise, which can in principle contribute with a high rate, are generally easily rejected in bolometers due to pulse-shape discrimination. In conclusion, while a generic source can be reduced by careful shielding, purification of materials, improvement of the noise figure, and anti-coincidence techniques, the random coincidence of $2\nu 2\beta$ events is a background hard to suppress, as it is related to the very presence of the isotope under investigation. The possibilities for decreasing this type of background to an acceptable level are discussed in the next section.

3 Pile-up rejection in scintillating bolometers

A cryogenic bolometer [28] consists of an energy absorber (a single diamagnetic dielectric crystal in $0\nu 2\beta$ applications) thermally linked to a temperature sensor that in some cases may be sensitive to out-of-equilibrium phonons. The heat signal, collected at very low temperatures (typically <20 mK for large bolometers), consists of a temperature rise of the whole detector determined by a nuclear event.

The majority of the most promising high $Q_{2\beta}$ -value (>2.5 MeV) candidates can be studied with the bolometric technique in the “source=detector” approach, combining high energy resolution and large efficiency [6, 7]. Ultra-pure crystals up to 100–1000 g can be grown with materials containing appealing candidates. Arrays of the single crystalline modules allow us to achieve total masses of the order of 100–1000 kg [14–16], which are necessary to explore the inverted hierarchy region.

An excellent choice for the bolometric material, as used in the Cuoricino and CUORE experiments [13, 14], consists of TeO_2 (tellurite) that has a very large (27 % in mass) natural content of the $0\nu 2\beta$ candidate ^{130}Te . In terms of background, the experience provided by TeO_2 searches [29] shows clearly that energy-degraded α particles, emitted by the material surfaces facing the detectors or by the detector surfaces themselves, are expected to be the dominant contribution in all high $Q_{2\beta}$ -value candidates, for which the signal falls in a region practically free of γ background. The α background component can be made negligible by using scintillating or in general luminescent (including Cherenkov light [12, 24]) bolometers. In fact, since the α light yield is generally appreciably different from the β/γ light yield at equal deposited energy, while the thermal response is substantially equivalent, the simultaneous detection of light and heat signals, and the comparison of the respective amplitudes, represents a powerful tool for α/β discrimination and therefore for α background rejection [8–10]. Scintillation photons are usually detected by a dedicated bolometer, in the form of a thin slab, opaque to the emitted light and equipped

with its own temperature sensor. The light absorber, normally a Ge, Si, or Si-coated Al₂O₃ slab, is placed close to a flat face of the main scintillating crystal.

A wealth of preliminary experimental results [11, 18–23] show that this method is effective and that α rejection factors even much better than 99.9 % can be achieved. Once this discrimination capability of scintillating bolometer is taken into account, a detailed background analysis, based on reasonable assumptions on internal radioactive contamination, shows that a residual background level of $\sim 10^{-4}$ counts/(keV·kg·y) can be safely assumed [22, 23], opening the opportunity to explore the inverted hierarchy region of the neutrino mass pattern. However, the random coincidences of $2\nu 2\beta$ events discussed in Sect. 2 must be kept under control. According to Eq. (8), the rate of $rc-2\nu 2\beta$ events is proportional to the time resolution of the detector. Therefore, the time properties of the signal from a cryogenic detector play a crucial role in this form of background.

The large mass (~ 800 g), high energy resolution ($\sim 3\text{--}4$ keV FWHM at 2615 keV) detectors developed for Cuoricino and CUORE [13, 14] represent a sort of paradigm for $0\nu 2\beta$ decay bolometers, inspiring other proposed experiments and related R&D activities. As temperature sensors, neutron transmutation doped (NTD) Ge elements are used, characterized by a high impedance (1–100 M Ω) and a high sensitivity ($-d \log R/d \log T \sim 10$). Other promising solutions for the thermal sensors have been used [17, 30–32], but for the moment only the energy resolution and the reliability provided by NTD Ge-based bolometers seem to be compatible with a large-scale $0\nu 2\beta$ experiment. In these devices, the NTD Ge thermistor is glued to the TeO₂ crystal by means of a two-component epoxy. Their time resolution is strictly related to the thermal-signal risetime.

The temporal behavior of the thermal pulse, and therefore its risetime, can be understood due to a thermal model for the whole detector, described elsewhere [33–36]. The model predicts that large mass detectors with NTD Ge readout have risetimes of the order of tens of milliseconds. This is confirmed experimentally in the Cuoricino detectors, which exhibited pulse risetimes of the order of ~ 50 ms [13]. Similar values are expected for any cryogenic bolometers with a volume of the order of 100 cm³ and based on NTD Ge thermistors. Faster risetimes could be observed if an important component of the energy reaches the thermistors in the form of athermal phonons, but this possibility depends critically on the nature of the main crystal and of the crystal-glue-thermistor interface. The most conservative approach consists in assuming the slow risetime evaluated and observed in TeO₂ bolometers.

The time resolution of the main crystal can be made substantially shorter than the risetime, taking advantage of the excellent signal-to-noise ratio expected at the $0\nu 2\beta$ energy [37], which is of the order of 2000 to 1 in TeO₂

crystals. (However, this high value is still to be proved for other bolometric materials relevant for $0\nu 2\beta$ decay.) Even though the time resolution proved shorter by a factor of 10 with respect to the present TeO₂ risetime values, and therefore around 5 ms, the background values reported in Table 2 should be multiplied by a factor 5, bringing them above 10^{-3} counts/(keV·kg·yr) for ¹⁰⁰Mo. The background due to random coincidence of $2\nu 2\beta$ events would then be dominant. The advantage of scintillating bolometers, which promise to keep the other sources around or below 10^{-4} counts/(keV·kg·yr) [22, 23], would be substantially compromised.

However, the simultaneous detection of light and heat which characterizes scintillating bolometers offers the possibility to control this problematic background source as well. In fact, a much faster risetime in the light-detector signal is expected, due to the much lower heat capacity of the energy absorber, which has now a mass of only a few grams at most. Following the bolometer thermal model [33–36], the light-detector risetime can be reduced to ~ 1 ms. Assuming a similar time resolution, the $2\nu 2\beta$ background contribution is in the ranges shown in Table 2, due to the fast response provided by the light detector.

The above discussion is simplified: the capability to discriminate two close-in-time events cannot be reduced to a single parameter such as the detector time resolution τ . In fact, it depends smoothly on the temporal distance between the two events and on the ratio between their two amplitudes as well. Furthermore, the pile-up discrimination capability is influenced by the signal-to-noise ratio in the light detector [37] and by the pulse shape and noise features. A complete analysis, the details of which will be reported elsewhere in a dedicated publication, has been performed. In this letter, we present the main results of this investigation and the most important conclusions.

An experiment based on modules of Zn¹⁰⁰MoO₄ crystals was considered. We have used pulse shapes and noise from a *real* light detector, of the same type as those described in [21, 22], coupled to a ZnMoO₄ scintillating crystal. The pile-up phenomenon was studied by generating light pulses with the observed experimental shape on top of experimental noisy baselines. In particular, pairs of pulses were generated with random time distances with a flat distribution up to 10 ms—in fact, the interarrival time distribution is practically constant over the [0, 10] ms range (this is the relevant time interval, since it allows us to fully explore the most problematic pile-up case, i.e., that occurring on the pulse risetime which is of the order of 3 ms). In Fig. 2, two pile-up emblematic cases (both with 3 ms time separation) extracted from the performed simulation are shown, along with a single pulse as a reference.

As a first step, we defined a 90 % efficiency in accepting a pulse from the light detector as a potentially good $0\nu 2\beta$

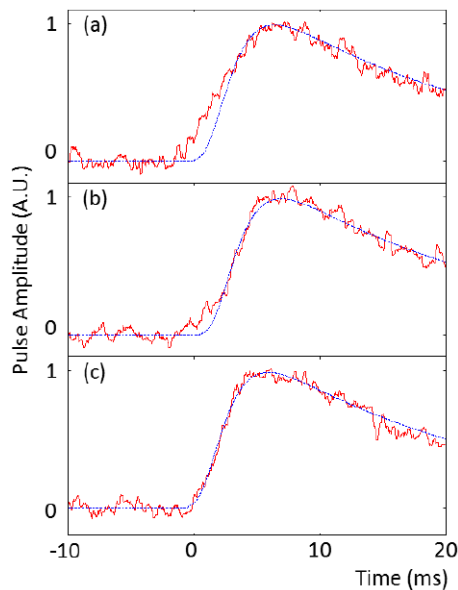


Fig. 2 Simulated piled-up pulses (*solid red lines*) using real pulse shape and noise from a working light detector coupled to a ZnMoO_4 scintillating bolometer: (a) pile-up of two pulses shifted by 3 ms with equal amplitude; (b) pile-up of two pulses shifted by 3 ms with amplitude ratio equal to 4 (the smaller pulse occurs first); (c) a single pulse. The typical single-signal pulse shape, obtained by fitting an average pulse, is plotted as well (*dashed blue lines*). In all cases, the signal-to-noise ratio is that expected for a $0\nu 2\beta$ signal. The difference in shape between piled-up and single pulses is small, especially for unequal amplitudes, but appreciable (Color figure online)

pulse using opportune signal filtering and three different pulse-shape indicators: (i) the risetime from 15 % to 90 % of the maximum amplitude; (ii) the χ^2 evaluated using an average pulse as a standard shape function; (iii) the pulse shape parameter defined in [38], which also uses a standard pulse-shape function. The rejection efficiency of piled-up pulses was then tested. In each pulse pair, the amplitude of the first pulse A_1 was extracted by sampling the $2\nu 2\beta$ distribution, while the amplitude of the second pulse A_2 was chosen as $Q_{2\beta}({}^{100}\text{Mo}) - A_1 + \Delta E$, where ΔE is a random component in the interval $[-5, +5]$ keV.

The generated pulse amplitudes were chosen so as to fix the signal-to-noise ratio at the level expected for a $0\nu 2\beta$ signal, i.e., of the order of 30, as shown in Fig. 2. In fact, the typical light energy collected by the light detectors in ZnMoO_4 scintillating bolometers realized so far is of the order of 1 keV for 1 MeV energy in the heat channel [20–23], while the typical RMS noise of the light detector can be conservatively taken as 100 eV, although values as low as 30 eV were observed [21].

The piled-up pulses generated in the simulation were analyzed with the mentioned pulse-shape indicators. Using the risetime (after low-pass filtering), an excellent pile-up rejection efficiency was obtained. A comparison between the risetime distribution for genuine single pulses and piled-up

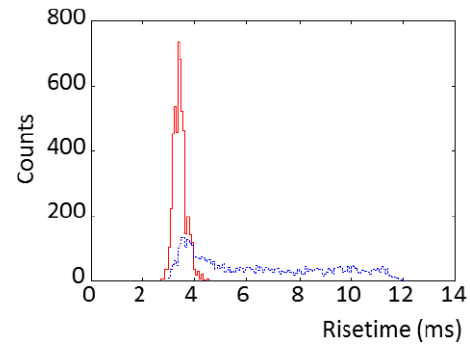


Fig. 3 Risetime distribution for two populations of 5000 generated events each. The *solid (red) line* refers to single pulses; the *dashed (blue) line* is obtained with piled-up pulses separated by a time distance uniformly covering the interval $[0, 10]$ ms, with amplitudes sampling the $2\nu 2\beta$ spectrum and adding so as to fall in the region of the $0\nu 2\beta$ expected peak (Color figure online)

pulses generated as described above is shown in Fig. 3. More quantitatively, the same procedure that retains 90 % of genuine single pulses rejects 80 %–90 % of piled-up pulses when their sum amplitude is in the region of $Q_{2\beta}$ and the difference between the arrival times of the two pulses covers uniformly the interval $[0, 10]$ ms. For example, the analysis of the sample reported in Fig. 3 excludes 83 % of piled-up pulses when accepting 90 % of good pulses. The other two indicators provide equivalent or even better results. However, we prefer here to consider conservatively the results obtained with the method of the risetime, as this parameter is an intrinsic property of each signal that does not require the comparison with a standard shape. This comparison in fact implies a delicate synchronization between the single pulse and the standard-shape pulse; this topic will be discussed in the aforementioned more complete work.

The results of the simulation show that the contribution to the background of the piled-up events is substantially equivalent to that obtained when assuming a time resolution τ of 1 ms in Eq. (9) (since 80 %–90 % of the pulses are rejected in the region of $0\nu 2\beta$ decay inside a pile-up relevant range of 10 ms), and therefore confirming the evaluation for ZnMoO_4 reported in Table 2.

We can thus conclude that light detectors at the present technological level are compatible with next-generation $0\nu 2\beta$ decay experiments based on ZnMoO_4 crystals with background in the 10^{-4} counts/(keV·kg·y) scale, confirming that this class of experiments has the potential to explore the inverted hierarchy region of the neutrino mass pattern [22, 23].

4 Conclusions and prospects

Random coincidence of $2\nu 2\beta$ events is an irremovable background source in large-scale 2β experiments using detec-

tors with slow response time, such as large mass cryogenic bolometers with NTD Ge readout.

Advancement of time resolution of cryogenic detectors plays a key role in suppressing the background. However, we have shown that the present technology is already compatible with searches at the sensitivity frontier. For further improvements, experimental efforts should be concentrated on the time properties of the light signal, which are potentially much faster than the heat pulses of a scintillating bolometer. Achieving a time resolution below 0.1 ms could make the background totally negligible, even for the difficult case of ^{100}Mo . This performance could be obtained by using sensors that are sensitive to out-of-equilibrium phonons or intrinsically fast [30–32].

A more direct way to decrease the pile-up effect is to reduce the volume of the main absorber (and increase correspondingly the number of array elements), on which the random coincidence rate depends quadratically, as shown in Eq. (9). Cryogenic detectors with space resolution could allow one to reduce the background further.

Acknowledgements The work of F.A. Danevich and V.I. Tretyak was supported in part through the Project “Kosmomikrofizyka-2” (Astroparticle Physics) of the National Academy of Sciences of Ukraine. The light detector results used for the pile-up simulation have been obtained within the project LUCIFER, funded by the European Research Council under the EU Seventh Framework Programme (ERC grant agreement n. 247115). The background study in ZnMoO_4 scintillating bolometers is part of the program of ISOTTA, a project receiving funds from the ASPERA 2nd Common Call dedicated to R&D activities.

Open Access This article is distributed under the terms of the Creative Commons Attribution License which permits any use, distribution, and reproduction in any medium, provided the original author(s) and the source are credited.

References

1. F.T. Avignone III, S.R. Elliott, J. Engel, *Rev. Mod. Phys.* **80**, 481 (2008)
2. A. Giuliani, *Acta Phys. Pol. B* **41**, 1447 (2010)

3. W. Rodejohann, *Int. J. Mod. Phys. E* **20**, 1833 (2011)
4. H.V. Klapdor-Kleingrothaus et al., *Eur. Phys. J. A* **147**, 12 (2001)
5. C.E. Aalseth et al., *Phys. Rev. D* **65**, 092007 (2002)
6. E. Fiorini, T.O. Niinikoski, *Nucl. Instrum. Methods Phys. Res. A* **224**, 83 (1984)
7. A. Giuliani, *J. Low Temp. Phys.* (2012). doi:[10.1007/s10909-012-0576-9](https://doi.org/10.1007/s10909-012-0576-9)
8. L. Gonzalez-Mestres, D. Perret-Gallix, *Nucl. Instrum. Methods Phys. Res. A* **279**, 382 (1989)
9. A. Giuliani, S. Sanguinetti, *Mater. Sci. Eng., R Rep.* **11**, 1 (1993)
10. A. Alessandrello et al., *Phys. Lett. B* **420**, 109 (1998)
11. S. Pirro et al., *Phys. At. Nucl.* **69**, 2109 (2006)
12. T. Tabarelli de Fatis, *Eur. Phys. J. C* **65**, 359 (2010)
13. E. Andreotti et al., *Astropart. Phys.* **34**, 822 (2011)
14. C. Arnaboldi et al., *Nucl. Instrum. Methods Phys. Res. A* **518**, 775 (2004)
15. F. Alessandria et al., [arXiv:1109.0494v1](https://arxiv.org/abs/1109.0494v1) [nucl-ex]. Accessed 2 September 2011
16. A. Giuliani et al., in *Proceedings of the Fifth International Conference Beyond 2010*, Cape Town, South Africa, 1–6 February 2010, ed. by H.V. Klapdor-Kleingrothaus, I.V. Krivosheina, R. Viollier (World Scientific, Singapore, 2011), p. 256
17. S.J. Lee et al., *Astropart. Phys.* **34**, 732 (2011)
18. C. Arnaboldi et al., *Astropart. Phys.* **34**, 344 (2011)
19. L. Gironi et al., *Opt. Mater.* **31**, 1388 (2009)
20. L. Gironi et al., *J. Instrum.* **5**, 11007 (2010)
21. J.W. Beeman et al., *J. Low Temp. Phys.* (2012). doi:[10.1007/s10909-012-0573-z](https://doi.org/10.1007/s10909-012-0573-z)
22. J.W. Beeman et al., *Phys. Lett. B* **710**, 318 (2012)
23. J.W. Beeman et al., *Astropart. Phys.* (2012). doi:[10.1016/j.astropartphys.2012.02.013](https://doi.org/10.1016/j.astropartphys.2012.02.013)
24. J.W. Beeman et al., *Astropart. Phys.* **35**, 558 (2012)
25. V.I. Tretyak, Yu.G. Zdesenko, *At. Data Nucl. Data Tables* **61**, 43 (1995)
26. H. Primakoff, S.P. Rosen, *Rep. Prog. Phys.* **22**, 121 (1959)
27. A.S. Barabash, *Phys. Rev. C* **81**, 035501 (2010)
28. A. Giuliani, *Physica B* **280**, 501 (2000)
29. M. Pavan et al., *Eur. Phys. J. A* **36**, 159 (2008)
30. A. Fleischmann et al., *AIP Conf. Proc.* **1185**, 571 (2009)
31. G. Angloher et al., *Astropart. Phys.* **31**, 270 (2009)
32. C. Nones et al., *J. Low Temp. Phys.* **151**, 871 (2008)
33. J. Zhang et al., *Phys. Rev. B* **57**, 4472 (1998)
34. A. Alessandrello et al., *Czechoslov. J. Phys.* **46-S5**, 2893 (1996)
35. M. Pedretti et al., *Physica B* **329–333**, 1614 (2003)
36. L. Foggetta et al., *Astropart. Phys.* **34**, 809 (2011)
37. H. Spieler, *Semiconductor Detector Systems* (Oxford University Press, London, 2005)
38. T. Fazzini et al., *Nucl. Instrum. Methods Phys. Res. A* **410**, 213 (1998)